Transcriptionally active chromatin recruits homologous recombination at DNA double strand breaks.

Aymard, F., Bugler, B., Schmidt, C. K., Guillou, E., Caron, P, Briois, S, Iacovoni, J.S , Daburon, V, Miller, K. M, Jackson, S. P, and Legube, G.

Supplementary Information file: Supplementary Figure 1-8 and Supplementary Table 1-4

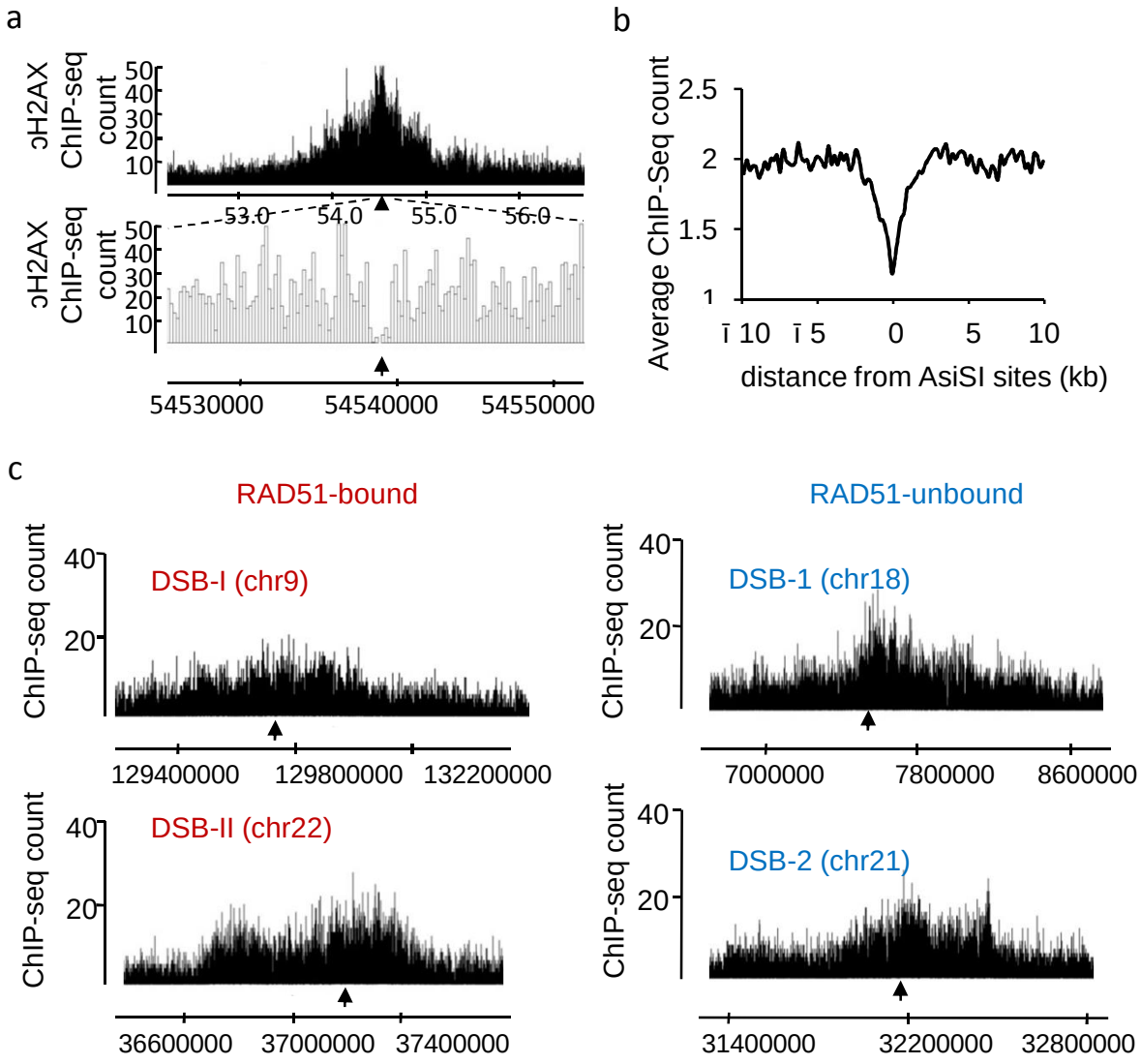

Supplementary Figure 1: γH2AX profile around AsiSI-induced DSBs.
ChIP-seq against γH2AX (Epitomics) performed in 4OHT treated DIvA cells. **a**. A representative γH2AX domain is presented (top panel, chromosome position are indicated in Mbp). A magnification of the γH2AX enrichment at the proximity of the DSB is shown (bottom panel, chromosomal positions are in bp). The DSB is indicated by an arrow. **b**. Average γH2AX signal on a 20kb window around each annotated AsiSI site on the human genome. **c**. The γH2AX signal obtained by ChIP-seq, around the DSBs presented Fig. 1b is shown. DSBs are indicated by arrows. RAD51-bound DSBs are indicated in red, and RAD51-unbound DSBs in blue.

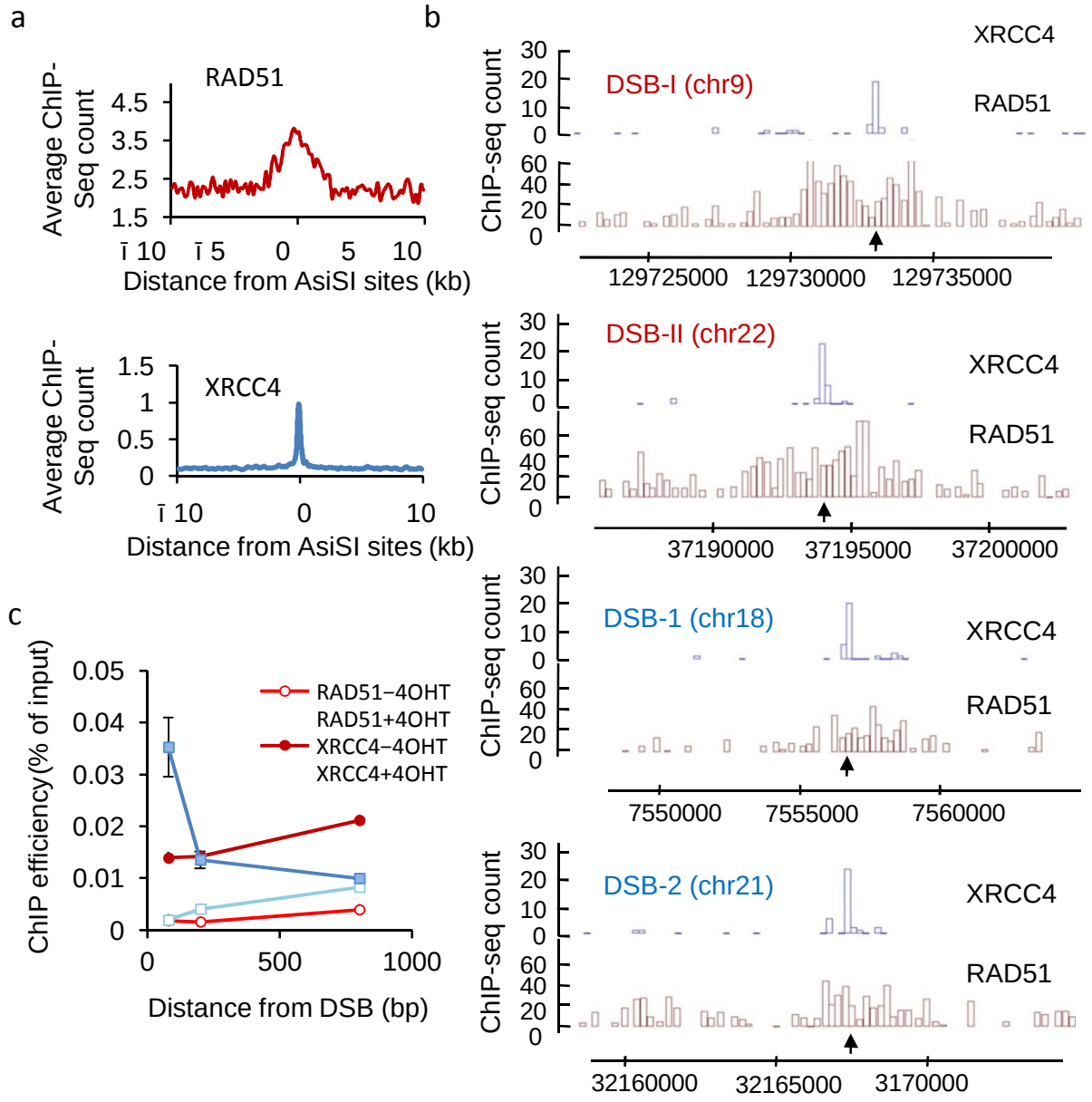

Supplementary Figure 2 : Binding of RAD51 and XRCC4 at AsiSI-induced DSBs.

a. Duplicate ChIP-seq experiment in 4OHT treated DIvA cells using an anti XRCC4 antibody (Abcam) or an anti-RAD51 antibody (Santa Cruz). The averaged XRCC4 (blue) and Rad51 (red) signal on 10kb around annotated AsiSI sites on the human genome are shown. **b**. Signals obtained around the four DSBs presented Fig. 1b are shown. Positions are indicated in bp. **c**. ChIP experiments performed in DIvA cells, treated (filled circles) or not (empty circles) with 4OHT, using an anti-XRCC4 antibody (blue) or an anti-RAD51 antibody (red). ChIP efficiencies (as percent of input immunoprecipitated) were measured by RT-qPCR at 80, 200 and 800bp from an AsiSI induced DSB (DSB-III). Mean and S.e.m (technical replicates n=4) of representative experiment is shown.

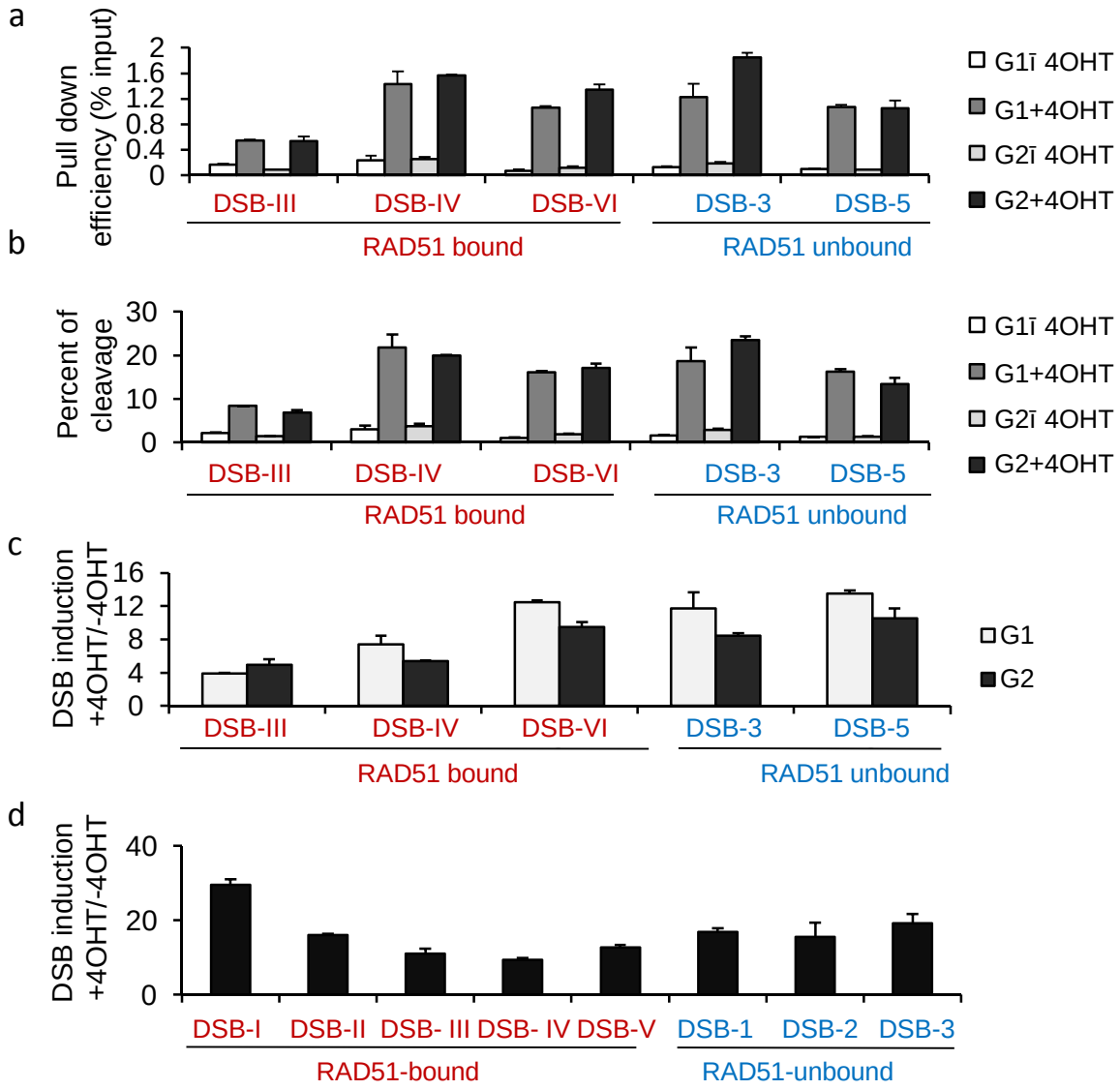

Supplementary Figure 3 : Measure of cleavage efficiency at selected AsiSI sites, throughout the cell cycle. Cleavage efficiency (using the protocol described in the online methods) was measured from untreated or 4OHT-treated cells by RT-qPCR for five AsiSI sites either identified as RAD51-bound or RAD51-unbound. The same representative experiment is presented in a, b and c. **a**. Raw qPCR data, as percent of input pulled down by the streptavidin purification are shown. **b.** The data presented in (a) were further normalized using an internal control constituted by *in vitro* AsiSI-digested plasmid added in the ligation reaction. This allows calculating the cutting efficiency at each specific sites as percent of cleavage (the *in vitro* digested plasmid representing the 100% cleavage). **c.** Ratios between treated and untreated cells are presented (using the normalized data presented in b). This last representation will be used throughout the manuscript. **d**. Pull own efficiency was measured by RT-qPCR for the eight AsiSI sites analyzed for the presence of ssDNA in Fig. 3a. Ratios between treated and untreated cells are presented. Mean and s.e.m (technical replicates, n=4) of a representative experiment is shown.

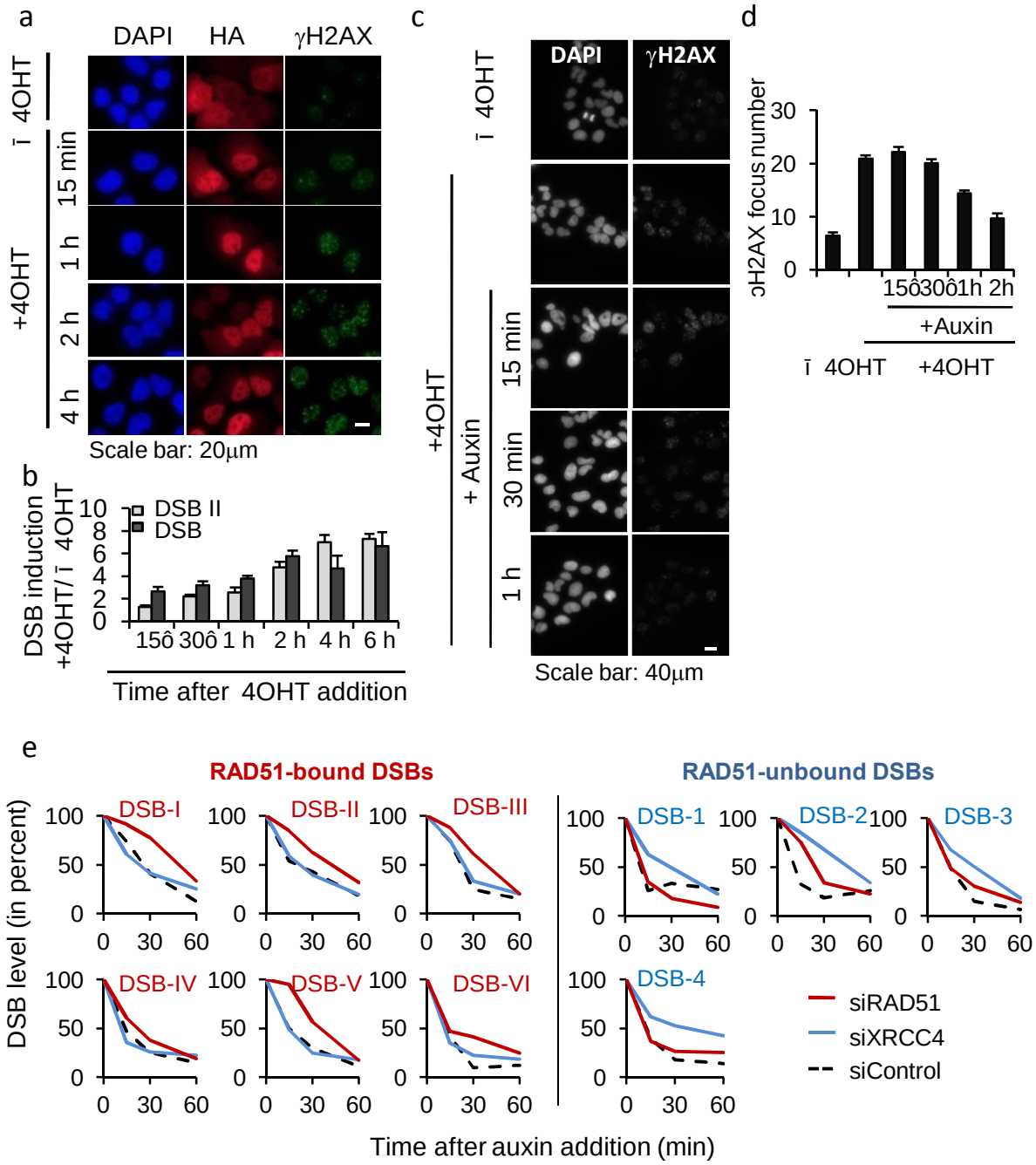

Supplementary Figure 4 : Kinetics of DSB induction and disappearance in the AID-DIvA cell line.
a. HA and γH2AX staining in AID-DIvA treated as indicated. **b.** Measure of cleavage efficiency, at two AsiSI-induced DSBs, in AID-DIvA cells treated as indicated. **c.** γH2AX staining in AID-DIvA cells treated (or not) with 4OHT for 4h and further incubated with auxin (or not) as indicated. **d**. γH2AX foci observed in AID-DIvA cells treated as in c, were counted using images aquired with an Array-Scan device. The mean and s.e.m (n=5, biological replicates, about 200 acquired nuclei per experiment) are presented. **e.** Repair analysis of AsiSI-induced RAD51-unbound (in blue, right panel) or RAD51-bound (in red, left panel) DSBs in AID-DIvA cells transfected with control, RAD51, or XRCC4. A biological replicate from Fig. 3f is shown.

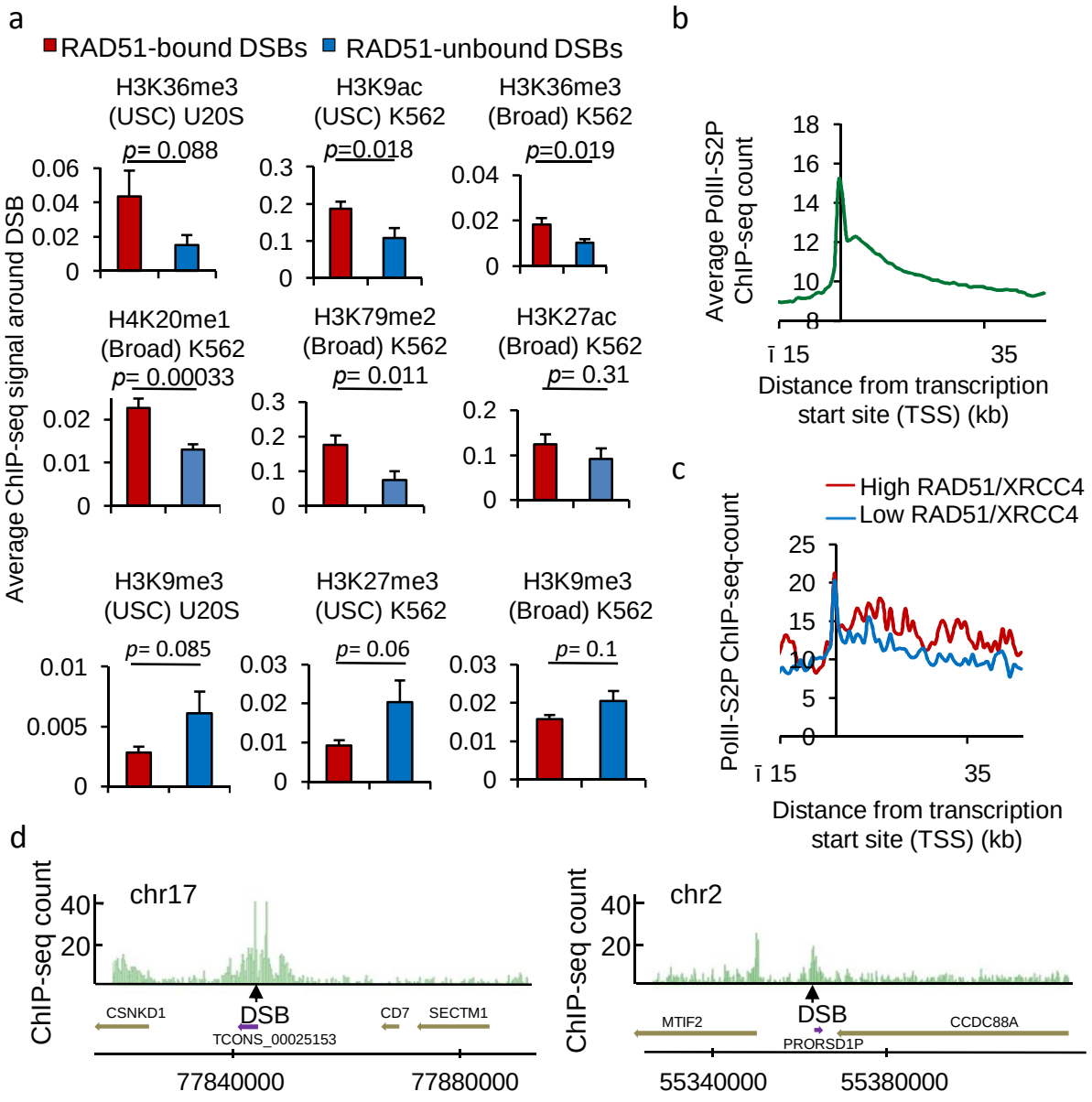

Supplementary Figure 5 : HR-prone DSBs are enriched in active chromatin marks and in PolII-S2P.
a. ChIP-seq data of various histones marks, associated with active (top and middle panels) or inactive (bottom panels) chromatin in U20S and K562 cells were retrieved from the ENCODE project, over 4kb surrounding each DSB from the RAD51-bound (red) and RAD51-unbound subsets (blue). The name of the Institute that generated the data are indicated in parentheses. The average and s.e.m are shown. *p* values (Mann-Whitney) are shown above each graphs. **b.** Average PolII–S2P signal obtained by ChIP-seq in DIvA cells, around the transcription start sites (TSS) of all genes from the human genome (hg18). **c**. Similar analysis than for Fig.4b except that all cleaved DSBs (100 best) were divided in two categories of 50 DSBs each based on their ratio RAD51/XRCC4. **d.** The Pol II–S2P signal obtained around two RAD51-bound DSBs, but far from any annotated gene (RefSeq, indicated in brown) are shown. DSBs are indicated by arrows, and positions are in bp. Feature from in lincRNA (large intergenic non coding RNAs) and TUCP (transcripts of uncertain coding potential) database (UCSC)(left panel), or from annotated pseudogene and non coding RNA (UCSC)(right panel) are indicated in purple.

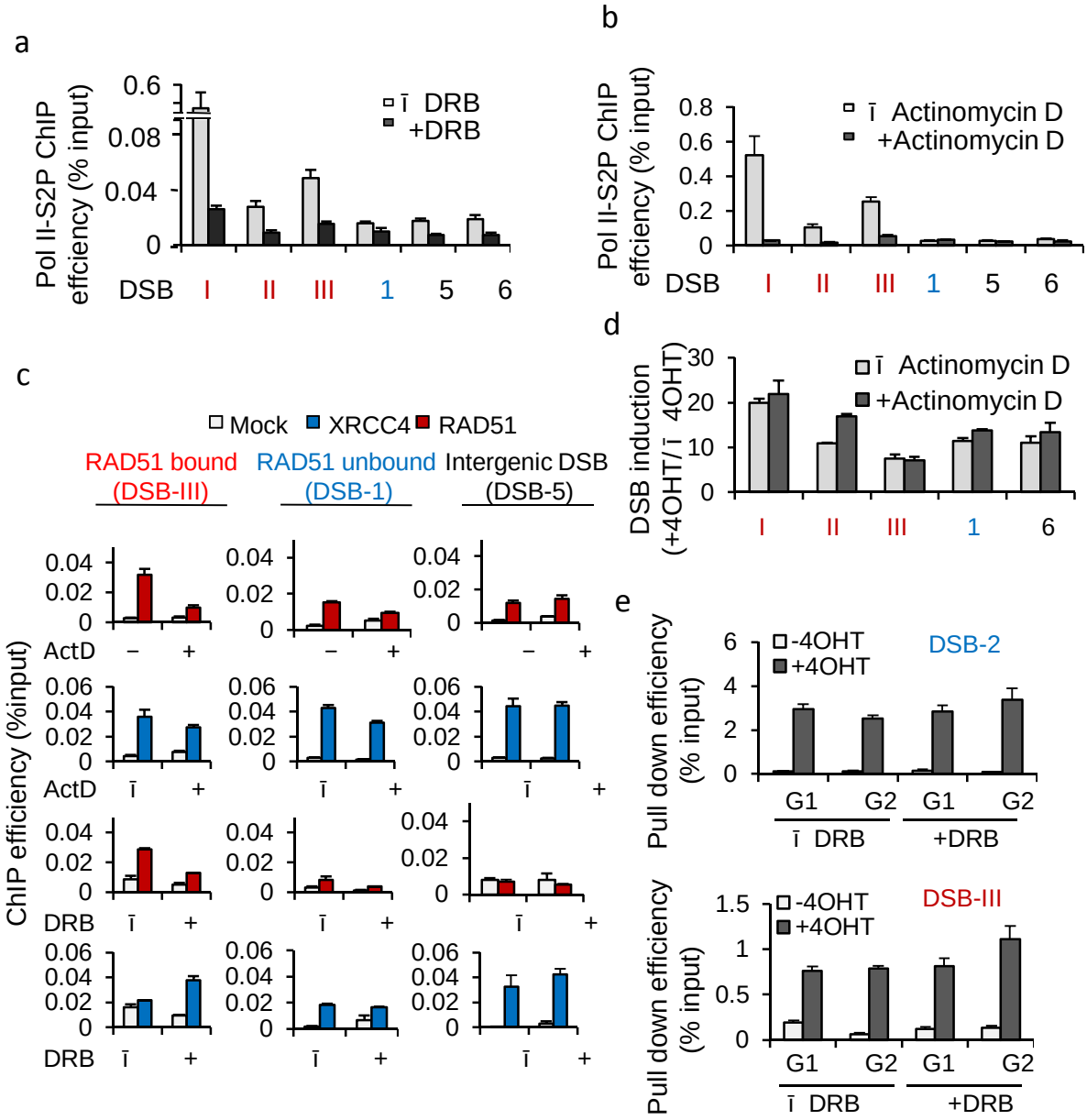

Supplementary Figure 6 : Effect of DRB and Actinomycin D on transcription, RAD51 binding and AsiSI-mediated break induction.

ChIP using a PolII-S2P antibody in 4OHT-treated DIvA cells incubated with DRB (**a**) or Actinomycin D (**b**) PolII-S2P levels were analyzed within a 1kb region around DSBs shown Fig. 4c-d, i.e. three RAD51-bound DSBs (DSB-I; -II; -III), one RAD51-unbound DSB (DSB-1), and two DSBs located far from any gene (DSB-5, -6). **c**. XRCC4 (blue) and RAD51 (red) ChIP in 4OHT-treated DIvA incubated with Actinomycin D or DRB as indicated. XRCC4 and RAD51 enrichments were respectively analyzed close to (<100bp) and at 800bp from selected DSBs, by RT-qPCR. The mean and s.e.m (n=4 technical replicates) of % of input immunoprecipitated for three DSBs (one RAD51-bound: DSB-III, one RAD51-unbound: DSB-1, and one intergenic: DSB-5) are shown. **d.** Analysis of cleavage efficiency in DIvA cells incubated with Actinomycin D (or not) (see online Methods). **e.** Analysis of cleavage efficiency in DIvA cells in G1 or G2 synchronized cells, and in presence or absence of DRB treatment as indicated, at an AsiSI site either identified as RAD51-bound (in red), or RAD51-unbound (in blue). Mean and s.e.m (n=4, technical replicates) of the raw qPCR data of a representative experiment, as percent of input pulled down by the streptavidin purification are shown.

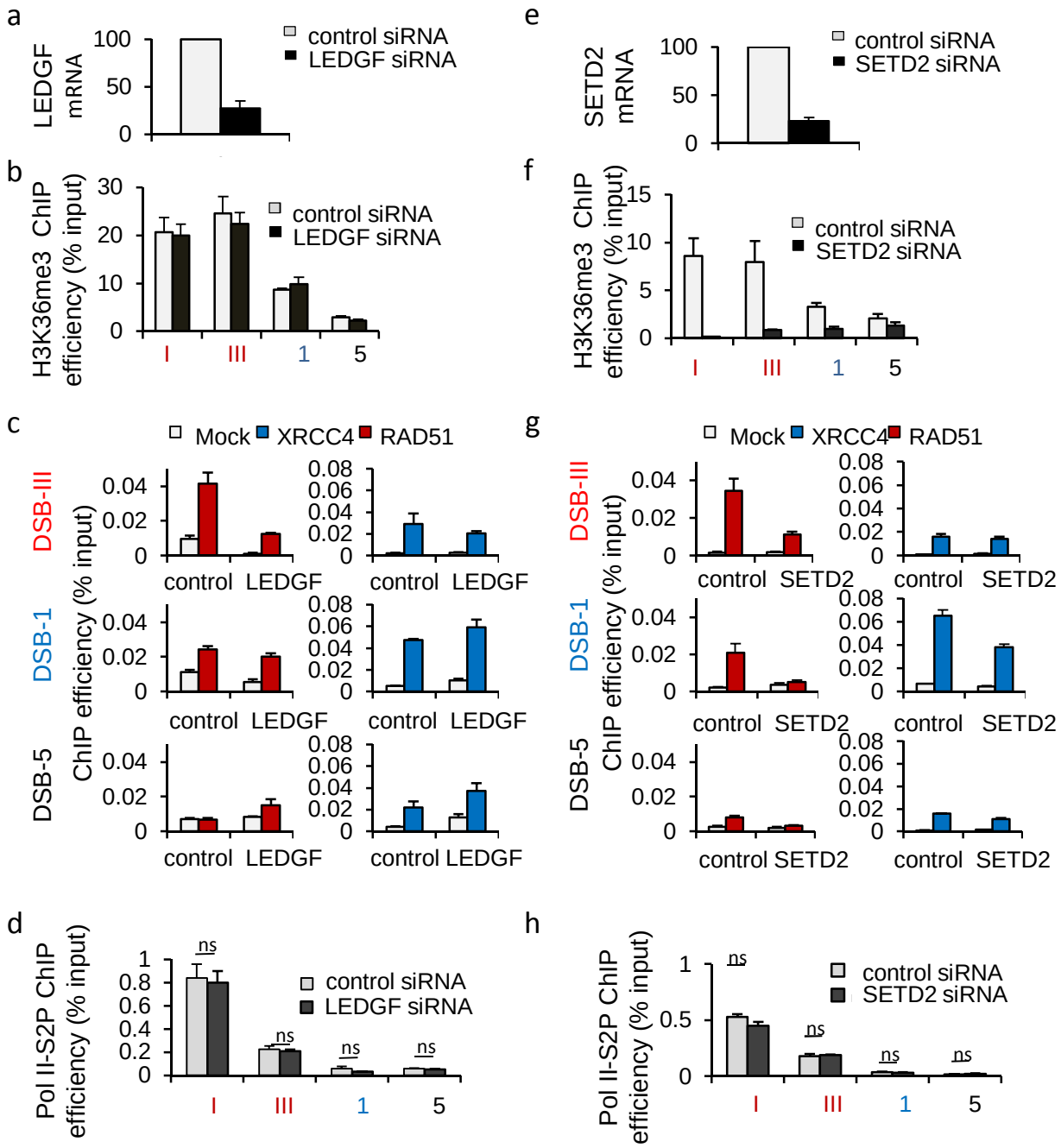

Supplementary Figure 7 : Effect of LEDGF and SETD2 siRNAs on H3K36me3, RAD51/XRCC4 and PolII-S2P levels.

DIvA cells were transfected using a control siRNA, a siRNA directed against LEDGF (a-d) or a siRNA directed against SETD2 (e-h). **a,e.** Relative mRNA level assessed by reverse transcription followed by qPCR. **b,f.** H3K36me3 ChIP analysed by qPCR at selected sites. **c,g** XRCC4 (blue) and RAD51 (red) ChIP after 4OHT-treatment respectively analyzed close to (<100bp) and at 800bp from selected DSBs. ChIP efficiencies (as % of input) are shown for 3 DSBs (RAD51 bound (DSB-III), RAD51 unbound (DSB-1), and intergenic (DSB-5)). The mean and s.e.m (n=4, technical replicate) of a representative experiment are presented. **d, h** PolII-S2P ChIP analyzed within a 1kb window around DSBs. The mean and s.e.m (n=4, technical replicate) of a representative experiment are presented. p values are indicated, ns non-significant (unpaired student test, two sided)

Figure 3b

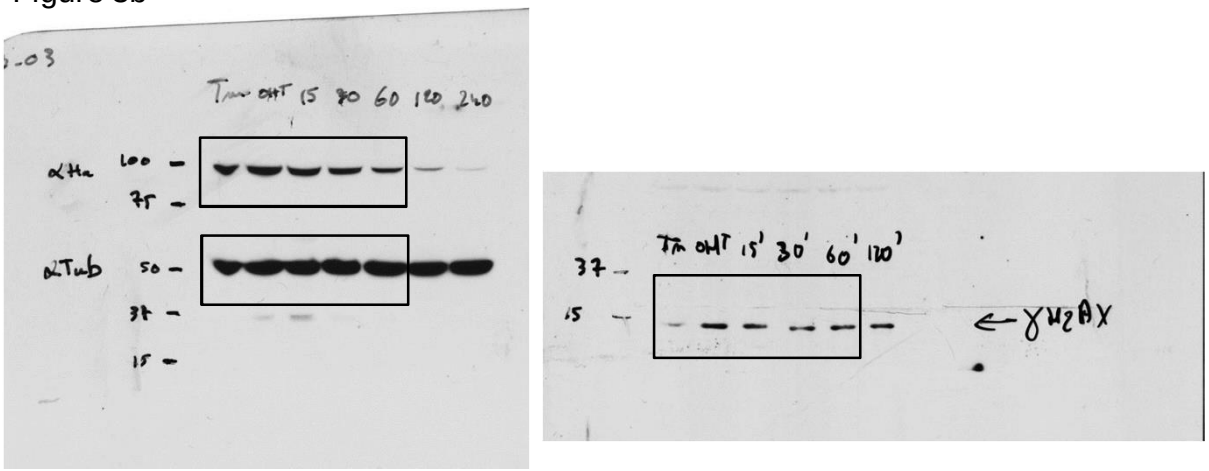

Figure 3e

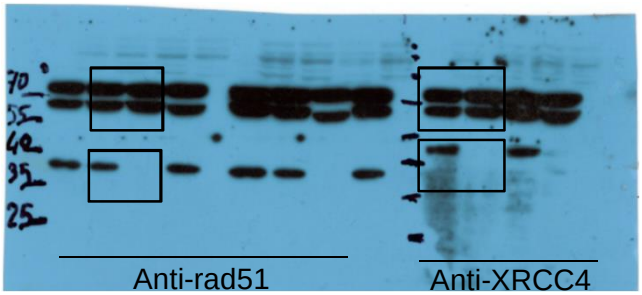

Supplementary Figure 8 : Uncropped blots presented on figure 3

a

DSB	Chromosome	*Asi*SI position	closest gene	Distance from the gene (bp)
	Chr1	19684735	CAPZB	942
	Chr2	55362598	CCDC88A	50907
	Chr3	52207196	ALAS1	Intragenic
	Chr7	2733591	GNA12	680
DSB-I	Chr9	129732985	PIP5KL1	83
	Chr9	129929222	PTGES2	Intragenic
	Chr9	136357891	RXRA	250
DSB-III	Chr17	5914679	WSCD1	Intragenic
DSB-IV	Chr17	77844122	CSNK1D	19959
	Chr17	77824392	CSNK1D	Intragenic
	Chr17	5330937	MIS12	515
	Chr17	4216265	UBE2G1	Intragenic
	Chr17	20886885	USP22	Intragenic
	Chr19	46595575	BCKDHA	Intragenic
	Chr19	2407588	LMNB2	Intragenic
	Chr19	2406985	LMNB2	Intragenic
	Chr19	2407086	LMNB2	Intragenic
DSB-V	Chr20	30409966	ASXL1	Intragenic
DSB-VI	Chr20	41520524	SFRS6	Intragenic
DSB-II	Chr22	37194040	KDELR3	Intragenic

b

DSB	Chromosome	*Asi*SI position	Closest gene	Distance from the gene(bp)
	Chr1	40747224	DEM1	Intragenic
	Chr2	207738966	KLF7	102
	Chr2	68238246	PNO1	267
	Chr2	43211836	ZFP36L2	91208
	Chr3	39825968	MYRIP	343
	Chr4	178600563	AGA	Intragenic
	Chr5	142765236	NR3C1	Intragenic
DSB-3	Chr6	90404901	LYRM2	Intragenic
	Chr6	50025535	DEFB133	414
	Chr6	135861034	MIR548H4	Intragenic
	Chr8	116749799	TRPS1	Intragenic
	Chr9	29202793	LINGO2	Intragenic
	Chr10	94040987	MARCH5	Intragenic
	Chr11	24475044	LUZP2	52
	Chr11	75203401	UVRAG	463
	Chr15	66899167	ANP32A	Intragenic
DSB-1	Chr18	7556705	PTPRM	613
DSB-4	Chr19	34711320	VSTM2B	Intragenic
DSB-2	Chr21	32167382	HUNK	121
	ChrX	72699821	CHIC1	Intragenic

Supplementary Table 1: Subset of RAD51-bound and RAD51-unbound AsiSI-induced DSBs.
AsiSI sites positions are indicated as well as the identity of the nearest gene (according the hg18 human genome). The sites indicated in blue are far from any annotated gene and were thus removed for the Pol II-S2P and H3K36me3 averaging analyses presented Fig. 4b and Fig. 6b. DSB-I to -VI and -1 to -4 used throughout the manuscript are indicated. **a**. RAD51-bound DSBs. **b**. RAD51-unbound DSBs.

	Forward	Reverse
Control	CAUGUCAUGUGUCACAUCUtt	AGAUGUGACACAUGACAUGtt
RAD51	CCAGAUCUGUCAUACGCUAtt	UAGCGUAUGACAGAUCUGGtt
XRCC4	AAUCUUGGGACAGAACCUAAAtt	UUUAGGUUCUGUCCCAAGAUUtt
SETD2	GUGAAGGAGUAUGCACGAAtt	UUCGUGCAUACUCCUUCACtt
LEDGF	CAGCCCUGUCCUUCAGAGAtt	UCUCUGAAGGACAGGGCUGtt

Supplementary Table 2: siRNA sequences used in this study.

	primer FW	primer REV
DSB-1_800bp	GGAGAAGTGGCAGGACAATG	CAAGGCAAATTTGGGGACTA
DSB-1_80bp	TCCCCTGTTTCTCAGCACTT	CTTCTGCTGTTCTGCGTCCT
DSB-1_gene	CATGCCTCAGAAACGTTGAA	GGTGCAGTGGTGCAATCATA
DSB-2_800bp	TTTTTGGGGGAAAGAGGTG	AGTGGGTGAGCCATTCAAAG
DSB-2_80bp	ATCGGGCCAATCTCAGAGG	GCGACGCTAACGTTAAAGCA
DSB-2_gene	TGCAGTTCTCCAATGACAGG	CATCTTTCAGGTGCTGGTCA
DSB-3_800bp	GGCACCTCAACAGGTAGCAT	GCCTCTCTTCGATGCTTTTG
DSB-3_80bp	GGAAGGAGGGGCTACTAGGG	GAAAGCCCCATTCAGTTTGA
DSB-3_gene	CAAAGATGACCACAGCCTCA	CACACCCCAAGAAAAGAGGA
DSB-4_800bp	CGTGGGGAAGTTAAGGAACA	CCCCATCACGTTAACCAAAC
DSB-4_80bp	AGGGTCGGGTTCTCTTTTGT	CCCGGTGCTAGGAGGAAT
DSB-4_gene	TTACTGTGTGCCACGCTCTC	CTCTTTTCTTGGGGGCTACC
DSB-5_800bp	GGGGAAATTGGGCATTAGTT	TTCGCCTCTTGGTTCTCTGT
DSB-5_80bp	GGTGCCCACAGCTCTCTATG	GAAGCCAGAGGAGTGTCCTG
DSB-6_800bp	GCTCAGTGTCTGGAAAATGGA	GCCTCTTGGGCTCTTCCTTA
DSB-6_80bp	TTCGACACCATCTCGGAACT	GATGCTCCTCGCTCACTACC
DSB-I_800bp	TATGGGACCAAGCGAGTAGG	GCCTCACACACACACCCATA
DSB-I_80bp	GTCCCTCGAAGGGAGCAC	CCGACTTTGCTGTGTGACC
DSB-I_gene	TGCAAGGCATTCGACAATAA	ATGGAAGCCATAATGCAAGC
DSB-II_800bp	GGGTATGGAGCTGCCTCTAA	GACAAAGATGGCTGGAGGAG
DSB-II_80bp	CCGCCAGAAAGTTTCCTAGA	CTCACCCTTGCAGCACTTG
DSB-II_gene	TGTGAGGGCTCAGTGAGATG	ACATTCCTCACCTGCCAAAC
DSB-III_800bp	GGGACAGCGCGTACTTTG	TCGCTAGGCCCAGCAGTT
DSB-III_200bp	GGGGCTTTTGGGAAAATTAC	AGCGACACTCTTGCCTCTG
DSB-III_80bp	CCGTCCGTTACGTAGAATGC	GGGCGGGGATTATGTAATTT
DSB-III_gene	CAGGCCGTTGAACAGGTTAT	TCAGCTGCAAAAACAGTTGC
DSB-IV_800bp	GAGGAACCATTCGGACAAGA	CTGACCAAGGAAGCCTCAAG
DSB-IV_80bp	GAGGAGCGCAGGACACTG	CCAATTAGAGACCACCCGTTT
DSB-V_800bp	GTCAGTATGGCCCCAGAGTC	ACGGCTGATGGACTTAGACG
DSB-V_80bp	CCTAGCTGAGGTCGGTGCTA	GAAGAGTGAGGAGGGGGAGT
DSB-V_gene	AAGCCACAGCCCACTAAAGA	GGCTGTCTCAAGCAAACCTC
DSB-VI_800bp	ACCCTTTGGCTGACCTTACC	TGAGGTTTTTGGTGGTGGTT
DSB-VI_80bp	GGTTTGGGTGTTTGGTTTTG	GCCCCCGAACCTCTAACTAA
DSB-VI_gene	AAAAGTCGCTCCCGGTAAAT	CCGATCAGACTTGGGCTTAG
DSB (fig. 3d, Fig.S 4b)	GATTGGCTATGGGTGTGGAC	CATCCTTGCAAACCAGTCCT
GBP1-TALEN_80bp	CCCAAACCTTCCATTTTCCT	GGTCAGAGGGGACACCTGTA
GBP1-TALEN_800bp	TTGCAGGATAGGACTCGTGA	GGCCAAACTTAGCAACCAGA

Supplementary Table 3 : oligonucleotides for RealTime Quantitative PCR used in this study.

	Primer FW_biotinylated	Primer REV_specific
Cleavage	CGCAAGCTTTAATACGACTCACTATAGGG	CCCTATAGTGAGTCGTATTAAAGCTTGCGAT
Resection_DSB-1	CGCAAGCTTTAATACGACTCACTATAGGG	CCCTATAGTGAGTCGTATTAAAGCTTGCGATCGCCAGCCCGCTC
Resection_DSB-2	CGCAAGCTTTAATACGACTCACTATAGGG	CCCTATAGTGAGTCGTATTAAAGCTTGCGATCGCGGTGGCGGCG
Resection_DSB-3	CGCAAGCTTTAATACGACTCACTATAGGG	CCCTATAGTGAGTCGTATTAAAGCTTGCGATCGCTCCTAGCCGC
Resection_DSB-I	CGCAAGCTTTAATACGACTCACTATAGGG	CCCTATAGTGAGTCGTATTAAAGCTTGCGATCGCCTGCGGGTCC
Resection_DSB-II	CGCAAGCTTTAATACGACTCACTATAGGG	CCCTATAGTGAGTCGTATTAAAGCTTGCGATCGCTAAGGAATGC
Resection_DSB-III	CGCAAGCTTTAATACGACTCACTATAGGG	CCCTATAGTGAGTCGTATTAAAGCTTGCGATCGCAGCGGTTTTA
Resection_DSB-IV	CGCAAGCTTTAATACGACTCACTATAGGG	CCCTATAGTGAGTCGTATTAAAGCTTGCGATCGCCAGACGCGGC
Resection_DSB-V	CGCAAGCTTTAATACGACTCACTATAGGG	CCCTATAGTGAGTCGTATTAAAGCTTGCGATCGCTAAGGAATGC

Supplementary Table 4: Double strand oligonucleotides used for cleavage and resection assay.
The 3' protruding end is underlined. Sequences specific for each site are indicated in red.